Geomorphology 317 (2018) 10–22

Contents lists available at ScienceDirect

Geomorphology

journal homepage: www.elsevier.com/locate/geomorph

Past ice stream and ice sheet changes on the continental shelf off the Sabrina Coast, East Antarctica

R. Fernandez [a,*,1], S. Gulick [a], E. Domack [b], A. Montelli [a,2], A. Leventer [c], A. Shevenell [b], B. Frederick [a,3], the NBP1402 Science Party

[a] Institute for Geophysics, Jackson School of Geosciences, University of Texas at Austin, Austin, TX 78758, USA
[b] College of Marine Science, University of South Florida, Saint Petersburg, FL 33701, USA
[c] Geology Department, Colgate University, Hamilton, NY 13346, USA

ARTICLE INFO

Article history:
Received 21 January 2018
Received in revised form 22 May 2018
Accepted 23 May 2018
Available online 24 May 2018

Keywords:
East Antarctic Ice Sheet
Glacial geomorphology
Mega scale glacial lineations
Grounding zone wedges

ABSTRACT

Our understanding of the response of the Antarctic ice sheet to climate and ocean changes requires the improvement of current ice-atmosphere-ocean models and the accurate determination of boundary conditions such as ice thickness and extent at key time intervals, so that satellite gravity observations and isostatic models can be adjusted. However, large portions of the Antarctic margin remain understudied or lack suitable data. One key area where data are lacking, is the Sabrina Coast portion of the East Antarctic Ice Sheet (EAIS) margin where the Totten Glacier, which has the largest ice discharge in East Antarctica, is accelerating, thinning and loosing mass at high rates. In this work, we present the results of the first geological and geophysical marine survey to the continental shelf offshore of the Dalton Ice Tongue and Moscow University ice shelf, east of the Totten Glacier. The data presented include multibeam swath bathymetry and multichannel seismic, focusing on the sea floor morphology and sedimentary section above a regional angular unconformity separating pre- and post-Miocene glacial strata. Sea floor scouring and iceberg keel marks on the outer shelf, associated with gullies on the upper slope indicate that ice expanded in the past and grounded ~5 km from the shelf edge at ~450–500 mbsl, extending ~155 km north of the current Moscow University Ice Shelf. A nearly 1000 m deep area in the inner-middle shelf, oriented NW with paleo-ice flow direction indicated by mega scale glacial lineations (MSGL) and drumlins, is interpreted as a cross shelf glacial trough. A series of geomorphic associations on the north-eastern side of the glacial trough includes glacial lobes, grounding zone wedges (GZW), glacial lineations and transverse ridges, which indicates slower ice, grounding line stabilization and collapse. These geomorphic associations are organized in 4 four sets representing different past ice-flow configurations reflecting changes in ice flow direction, grounding line position, location of fast and slow ice areas, and retreat pattern. Some of the geomorphic features identified are compatible with the presence of an organized subglacial drainage, and others are with rapid grounding line collapse. A well-preserved series of GZWs occurring at different water depths implies they were formed during different glacial stages or cycles. The inferred diminishing ice thickness for consecutives GZWs indicates that the margin of the Antarctic ice sheet evolved to a less extensive coverage of the continental shelf through successive glacial stages or cycles.

The identification of different ice flow configurations, evidence of subglacial water and past ice margin collapse indicates a dynamic ice sheet margin with varying glacial conditions and retreat modes. We observe that some of the described morphological associations are similar to those found in the Amundsen sea sector of the West Antarctic Ice Sheet (WAIS) where they are associated with ice sheet and ice stream collapse. Although further studies are needed to assess the precise timing and rates of the glacial processes involved, we conclude that there is enough evidence to support the hypothesis that the EAIS margin can behave as dynamically as the WAIS margin, especially during glacial retreat and icesheet margin collapse.

1. Introduction

The East Antarctic Ice Sheet (EAIS) contains ~53 m of sea level equivalent ice volume, ~19 m of which is grounded below sea level and thus susceptible to mass loss processes related to ice-ocean interactions such as termini and basal-ice melting, calving, and sea level rise, which can result in ice sheet instability and grounding line retreat (Lythe et al., 2001; Golledge et al., 2015; Fretwell et al., 2012; DeConto

* Corresponding author.
E-mail addresses: rfernandez@ing.uchile.cl, r.f@ig.utexas.edu (R. Fernandez).
[1] Present Address: Departamento de Geología, Universidad de Chile, Santiago, Chile Plaza Ercilla 803, Santiago, Region Metropolitana, Chile. Tel.: +56 9 40433216 (cell), +56 2 9784123 (office), +1 512 9617075 (US, online).
[2] Present Address: Scott Polar Research Institute, University of Cambridge, Cambridge, CB2 1ER, UK
[3] Present Address: Department of Geology, University of Kansas, Lawrence, Kansas, 66045, USA

https://doi.org/10.1016/j.geomorph.2018.05.020
0169-555X/

and Pollard, 2016). Despite its potential to influence global sea level, the exact magnitude, rate, and timing of the EAIS response to past and current atmospheric and oceanic changes remain uncertain (Gulick et al., 2017). In particular, the sign and trend of the EAIS mass balance is still a matter of debate owing to the difficulty of estimating the net mass change in the continental interior, the feedbacks between ice flow and ice-bed conditions and the complex ice flow dynamics and mass loss processes at the margin of the ice sheet (e.g., Hanna et al., 2013; Ivins et al., 2013; Zwally et al., 2015; Lenaerts et al., 2016). Some estimates indicate that ocean-heat driven basal melt under ice shelves and cavities of the EIAS accounts for almost half of the current mass loss rate, the rest corresponding mostly to calving (e.g., Rignot et al., 2013; Rintoul et al., 2016). However, recent observations (Lenaerts et al., 2016) and analysis of the last decade of aerial photographs and satellite data (Kingslake et al., 2017) indicate that the margin of the EAIS is also sensitive to rising atmospheric temperatures, which could lead to widespread ice shelf instability and breakup. The eventual breakup of ice shelves in the EAIS could subsequently lead to an increase in ice flux to the termini as observed after the breakup of Larsen A and B ice shelves (Rott et al., 2002; Rignot et al., 2004; Scambos et al., 2004), which would add to the current rates of ice mass loss and sea level rise.

Improvement of integrated ice sheet and climate models requires the accurate determination of boundary conditions such as ice thickness and extent at key time intervals so that satellite gravity observations and isostatic models can be adjusted (Hanna et al., 2013; Mackintosh et al., 2014). One such time interval is the termination of the last glacial cycle when global temperatures and sea level rose rapidly while the Antarctic Ice Sheet retreated from the continental shelf (RAISED, 2014). However, two major challenges to overcome are that large portions of the Antarctic margin remain understudied or lack suitable data (e.g., Mackintosh et al., 2014). One key area where data are lacking is the Sabrina Coast portion of the EAIS margin (Mackintosh et al., 2014) where the Totten Glacier, which has the largest ice discharge in East Antarctica, is accelerating and thinning (Li et al., 2016).

The stability and likelihood of collapse of the Antarctic Ice Sheet glaciers strongly depends on the ice-bed coupling near the grounding line, which controls the thickness and floatability of the ice sheet margin (Pingree et al., 2011). In the few areas that have been studied along the East Antarctic margin, the inner shelf is characterized by a deep rugged sea floor, believed to be mostly bedrock, which transitions to a smoother and shallower sedimentary substrate, forming a landward-sloping continental shelf (Leventer et al., 2006; Beaman et al., 2011; Mackintosh et al., 2011; O'Brien et al., 2016). This configuration of the continental shelf implies that during glacial times, the margin of the EAIS would have flowed on a bed of changing downstream conditions, including decreasing rugosity, basal drag, and depth. This sea floor configuration is observed in other regions of the Antarctic margin, such as in the continental shelf areas of the Western Antarctic Ice Sheet (WAIS) (e.g., Evans et al., 2006; Jakobsson et al., 2011) and the Antarctic Peninsula Ice Sheet (APIS) (e.g., Wellner et al., 2006; Lavoie et al., 2015); however, currently data are insufficient to estimate its prevalence for the EAIS.

Subglacial water may play a critical role dictating basal boundary conditions during advances onto and/or retreats from the continental shelf (Lowe and Anderson, 2003; Graham et al., 2009; Smith et al., 2009; Nitsche et al., 2013; Witus et al., 2014). Geophysical surveys of interior and coastal Antarctica reveal complex subglacial hydrologic systems in some East Antarctic locations (Wingham et al., 2006; Young et al., 2011; Wright et al., 2012; Aitken et al., 2014, 2016). However, direct evidence linking past and present subglacial hydrologic changes and ice dynamics is sparse (Stearns et al., 2008; Young et al., 2011; Siegfried et al., 2016). Whether or not subglacial water might play a role influencing ice dynamics in East Antarctic marginal environments is still unknown, but the general concern about the stability of the Antarctic ice sheet under current conditions of a changing climate and ocean requires that this possibility be investigated.

Here we present the results of the first geological and geophysical marine survey (NBP1402) to the inner and middle continental shelf offshore of the Dalton Ice Tongue and Moscow University ice shelf, east of the Totten Glacier (Fig. 1). The data presented include multibeam swath bathymetry and multichannel seismic, focusing on the sea floor morphology and sedimentary section above a regional angular unconformity separating a sequence of dipping strata that include preglacial through late Miocene stratified rocks with internal erosional features consistent with bed erosion under polythermal-glacial conditions and late Miocene to recent strata with internal seismic architecture consistent with polar-glacial conditions; the description and interpretation of the seismic section below this unconformity are presented in Gulick et al. (2017). This area is of special interest since the Totten Glacier is experiencing the largest ice mass loss rate in East Antarctica today (Chen et al., 2009; Rignot et al., 2009; Pritchard et al., 2012), and the area is seaward of the large Aurora Subglacial Basin where a complex subglacial hydrological system has been identified, including numerous subglacial lakes (Siegert et al., 2005; Young et al., 2011; Wright et al., 2012; Aitken et al., 2016). We describe a complex of seafloor features on the continental shelf that provide evidence that the sea floor was modified in the past by glacial processes, although this region is presently free of grounded glacial ice. In addition, these features indicate that in the past, different ice flow configurations and variable ice dynamics characterized the evolution of the paleomargin of the EAIS in our study area. Specifically, we discuss evidence of glacial erosion and deposition, of periods of fast ice flow and grounding line stabilization, of subglacial water, and of ice stream and ice sheet collapse. Our interpretations build upon the knowledge of similar geomorphic features described elsewhere in Antarctica and other glaciated regions and provide the first evidence of dynamic changes occurring in the margin of this sector of the EAIS.

2. Methods

Bathymetry and seismic data were collected as part of the 2014 RVIB Nathaniel B. Palmer (NBP) marine geology and geophysics cruise NBP1402 in the Dalton Ice Tongue polynya, just east of the Totten Glacier terminus and north of the Moscow University Ice Shelf (MUIS; Fig. 1). Swath mapping was conducted using the RV/IB N.B. Palmer's hull-mounted Simrad EM120 multibeam sonar system, which consists of 120 beams that use a 12 kHz source. Post-cruise, data were processed using Caris and Fledermaus software. Artifacts and bad pings were edited and gridded three-dimensional bathymetry data sets produced for geomorphological analysis. Gridded bathymetry data were imported into ArcMap 10.2.2 to map geomorphological features and to calculate magnitude of slopes, slope direction, and bathymetric profiles. Subsets of bathymetry data were stacked for statistical analyses using a Matlab code written by the authors to analyze gridded bathymetry data and to produce descriptive statistics and profiles. The interpretation of sea floor features was done by comparison with similar features described elsewhere in Antarctica and with the identification of associations of features, cross and cut relationships, and the simple assumption that deeper glacial features correspond to thicker ice conditions, which is expected for marginal areas of marine ice sheets. Multichannel seismic (MCS) data were acquired with dual generator–injector (GI) air guns and a 100 m-long gel-filled streamer (75 m active) with 24 channels with a spacing of 3.125 m. The true positioning of the guns and the streamer was obtained by correcting the ship GPS data with their relative position in respect to the receiver antenna and by a simple geometry model for the streamer using a proprietary Matlab code. The MCS data processing included prestack bandpass filtering and spherical divergence correction, deconvolution of the resulting signal to isolate the earth response (predictive, effective source wavelet and/or Hilbert transform deconvolution), trace balancing, normal moveout correction, stacking and dip moveout, and migration in the frequency-wavenumber domain. The final processed sections were visualized and studied

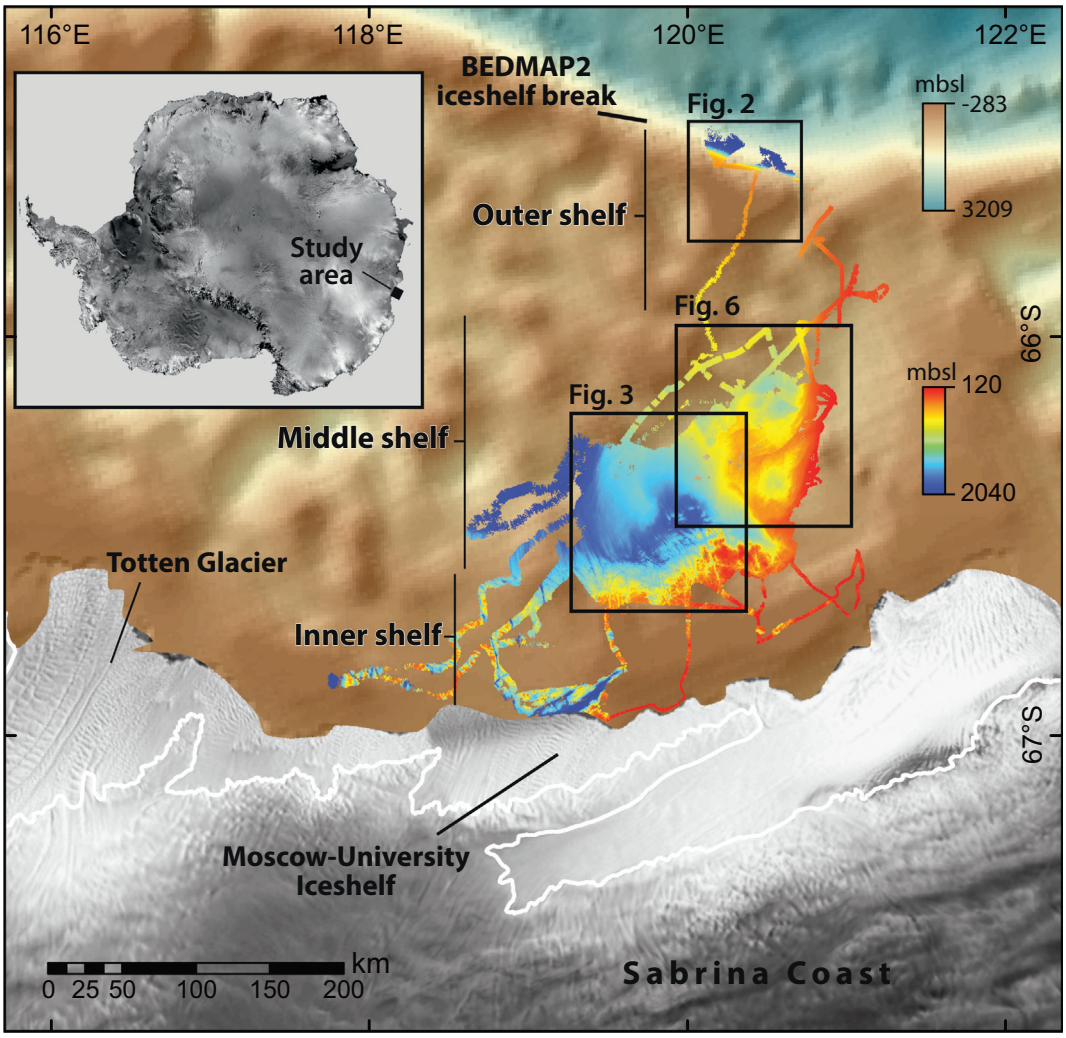

Fig. 1. Location of the study area. Brown to light blue color scale represent water depths according to the BEDMAP2 model (Fretwell et al., 2013). The Rainbow color scale represent the multibeam bathymetry acquired for this work. Antarctic image from the RADARSAT-1 Antarctic Mapping Project (RAMP) (Jezek and RAMP Product Team, 2002). Distinction between inner, middle, and outer shelves is based on sea floor morphology (Section 3) similar to other parts of the Antarctic margin (Anderson, 1999).

in Landmark software. The seismic data were used to support the morphological analyses and to provide additional constraints on past glacier behavior.

3. Results

3.1. Outer shelf

The shelf break was mapped in a small area ~155 km north of the Moscow-University Ice Shelf (MUIS) and occurs at water depths ~450–500 m and about 5–7 km north from where it appears to be located in the BEDMAP2 model (BEDMAP2; Fretwell et al., 2013; Fig. 2). We note that for water depths >~900 m in the middle and outer shelf, the BEDMAP2 modelled bathymetry (Fretwell et al., 2013) generally agrees with our multibeam bathymetry; but the fit is relatively poor for shallower depths (S01). A change in slope from steeply seaward to slightly landward occurs at 430–480 m water depth and about 5 km south of the shelf break in an area characterized by iceberg furrows and an asymmetric promontory with the steepest slope facing landward (Fig. 2). The upper continental slope is characterized by V-shaped gullies with ~40–60 m of relief (Fig. 2), which were mapped for about 30 km.

3.2. Middle shelf

Geomorphic evidence supporting the past existence of grounded ice on the continental shelf comes from the middle and inner shelf areas (Fig. 1). We identified a sharp geomorphological transition from a rugged and deeply incised sea floor in the southern parts of the study area toward a streamlined, smoother, and shallower sea floor, occurring ~80–100 km north from the current coastline (Fig. 3). This transition follows a NNE direction, parallel to the coastline and to a promontory that runs roughly parallel to the ice sheet grounding line according to the BEDMAP 2 model (S01; Fretwell et al., 2013). We define the inner-middle shelf boundary as this geomorphological transition between rugged and smooth/streamlined sea floor (Figs. 1, 3), which corresponds, according to our seismic imaging, to the limit between bedrock- (inner shelf) and sediment-dominated seafloor (middle shelf).

Seismic data show that the observed sea floor features that characterize the middle shelf are constructed or shaped within a sedimentary sequence that overlies the erosional unconformity and stratified seaward-dipping strata that represent prepolar ice sheet Meso-Cenozoic sediment accumulation in the Antarctic margin (Fig. 4; Gulick et al., 2017). The thickness of the unit above the unconformity is highly variable but locally can reach up to 100 m

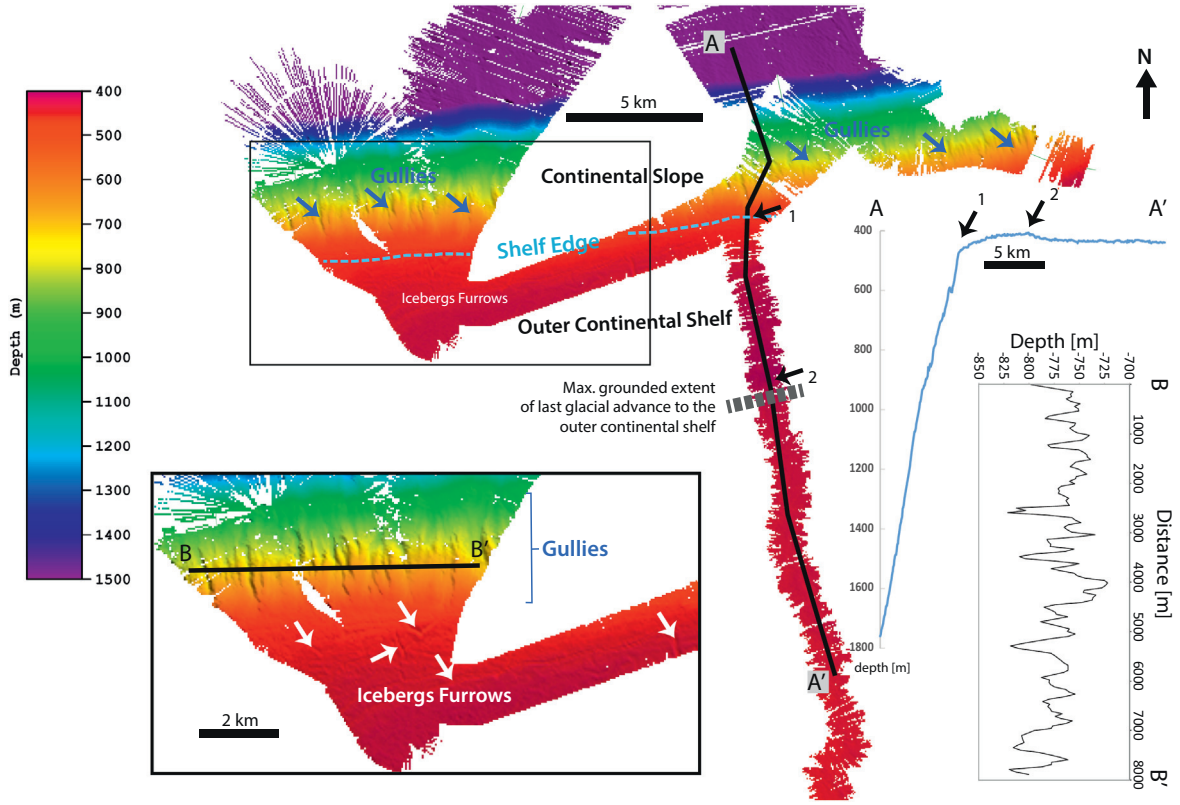

Fig. 2. Bathymetry of the outer shelf and continental slope area, indicating main geomorphological features including gullies and iceberg furrows. Profile A-A′, located N-S across the outer shelf and the upper slope, shows the position of the shelf break (1) and of a proposed grounding line feature (2). Profile B-B′ shows the relief of the upper slope gullies described in the text, which are typically 25–50 m deep.

or more in the most ice proximal areas and is directly correlated with the relief of the morphological elements observed on the seafloor; seismic images show that this unit is largely composed of chaotic or transparent facies separated by irregular and isolated reflectors (Fig. 4). In the following sections we describe the most conspicuous sea floor features.

3.2.1. The deep streamlined middle shelf seafloor

3.2.1.1. Megascale glacial lineations and drumlins. On the deepest parts of the middle shelf, the sea floor morphology is characterized by several types of streamlined bedforms. Seaward from the rugged bedrock area, a series of approximately north-south ridges and grooves with amplitudes varying between 5 and 25 m and crest-to-crest spacing ~300–400 m was mapped (Fig. 3). Although we have limited coverage of the shelf, the existence of parallel ridges with consistent strike across different bathymetry swaths suggests that they continue for at least ~10 km, implying elongations >25:1. The geometry of these ridges (amplitude, spacing, elongation ratio) and general appearance is consistent with mega-scale glacial lineations (MSGL) described elsewhere on the Antarctic margin (e.g., Antarctic Peninsula, Amundsen Sea) where they are associated with fast ice flow (Heroy and Anderson, 2005; Wellner et al., 2006; Ó Cofaigh et al., 2007; Graham et al., 2009) and will be referred as such (MSGL; Fig. 3). The MSGLs initiate in an area dominated by drumlins (drumlins field), which occur where the transition from bedrock- to sediment-dominated seafloor was mapped (Figs. 3, 5). The drumlins field occupies a narrow (<10 km) and elongated band (>60 km) where seismic images show that at least part of the drumlins are constructed around a bedrock core (Fig. 4). Maximum drumlin height is 10–40 m, but locally the relief is augmented by the prolongation of channels from the bedrock-dominated sea floor area so that ridge-to-groove height can reach up to 80 m. Because drumlins transition into MSGLs, length and elongation ratios are difficult to estimate for most of them; but in a subset where they can be traced, values are commonly 2–4 km and 5:1 to 10:1 respectively, well within the range for similar features observed on continental shelf areas of West Antarctica (e.g., Wellner et al., 2006; Clark et al., 2009; Spagnolo et al., 2011; Maclachlan and Eyles, 2013).

3.2.1.2. Glacial lobes. Superimposed on the MSGLs is a distinctive bedform complex 22 km wide and at least 30 km long, found below 600 m of water depth (Fig. 3). This bedform complex consists of a stacked set of ~N10E oriented lobes (LO1 through LO8; Fig. 3) with roughly parabolic shapes that appear to have cross-cutting relationships in plane view (Fig. 3) and stepwise boundaries in sectional view (Fig. 5). We refer to the individual features as *glacial lobes* and to the whole group of lobes as *a glacial lobes complex*. Seismic images show that the glacial lobes complex consists of a stack of seismically transparent or chaotic and partially stratified units separated by erosional unconformities (Fig. 4). Units lower in the stratigraphic sequence have an aggradational geometry, while those higher in the sequence reveal a progradational geometry with reflectors from upper units downlapping onto top reflectors from lower units (Fig. 4). The internal seismic architecture and morphological relationships between units enables us to establish their relative age, with the shallowest, smallest, and southernmost unit being the youngest and with the deepest, partially visible unit being the oldest (Fig. 3).

The geometry of the glacial lobes is better observed on their downstream side where they show distinctive <10–30 m stepwise and arcuate borders (Figs. 3, 5). The upstream side of the glacial lobes complex coincides with the initiation of the MSGLs and the drumlins field just north of where the rugged bedrock dominates the sea floor (Figs. 1, 3). The apparent surface of the lobes is characterized by glacial lineations formed by elongated ridges and grooves, generally 1–5 m

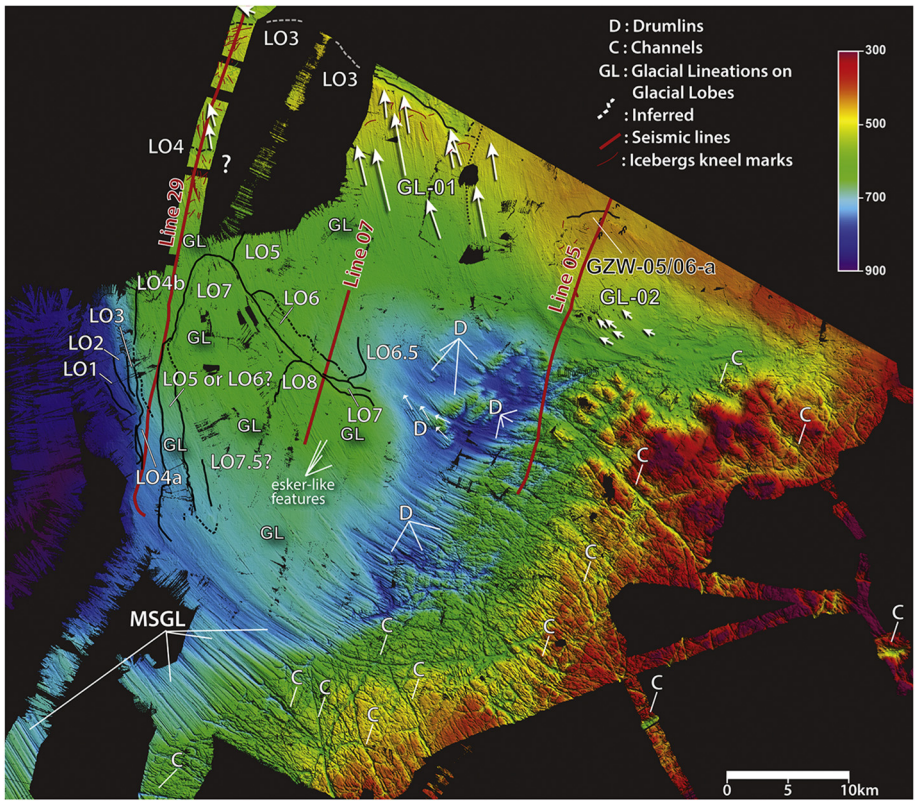

Fig. 3. Bathymetry of the inner shelf (rugged SE part; red-purple to green colors) and deeper middle shelf areas (NW part; deep blue and light green colors) indicating the main geomorphological features. White arrows indicate the inferred ice flow direction based on the orientation of glacial lineations. Red lines show the location of the seismic lines shown in Fig. 4. Black lines show the boundary of glacial lobes (Section 4.2) and are labeled LO01 - LO08 from deeper to shallower in the sedimentary section.

high and 100–300 m spacing, with slightly eastward bends in the downstream direction and better preservation on the upper/younger lobes (Fig. 5). On the top glacial lobe (LO8; Fig. 3), a set of glacial lineations has a peculiar appearance, showing positive relief (<5 m high), bifurcation, and shape changes along their length (Fig. 5).

The nature of the contact between the underlying MSGLs and the glacial lobe complex (i.e. whether or not it is erosive or concordant) was not completely resolved, but the fact that the seismic data show several erosional unconformities within this complex suggest that the glacial lobes were constructed by at least partially eroding the MSGLs. The following observations indicate that the glacial lobes complex was constructed subsequent to and under different glacial conditions than the MSGL. Glacial lineations on the surface of the glacial lobes are oblique to the main MSGLs direction. Some drumlins immediately south of LO8 (Figs. 3, 5) obliquely overprint larger ones and are parallel to the glacial lineations on LO8 (Fig. 5). Hence, we infer that ice flow direction during the formation of LO8 (Fig. 5) was oblique to the direction of ice flow when the older drumlins and MSGL were being formed.

3.2.2. The shallow middle shelf

The most conspicuous morphological feature in the shallow middle shelf area, which extends northeast of the glacial lobe complex at water depths ~270–540 m, corresponds to a set of seven elongated and arcuate NE-ENE wedges that are oblique or nearly perpendicular to the MSGLs (Figs. 4, 6). The wedges are asymmetrical with the steeper slopes to the NW, which is roughly the downstream direction of the MSGLs. Seismic data show that these wedges are constructed above the regional erosional unconformity that separate the Mesozoic-Cenozoic strata from the younger glacial sedimentary sequence (Fig. 4). The internal architecture shows progradational geometries near the downstream side, while the top (gentler slope face) is characterized by aggradational reflectors over mostly chaotic or transparent seismic facies (Fig. 4). Based on their morphology and similarity with features described elsewhere (e.g., Batchelor and Dowdeswell, 2015), we interpret these arcuate, asymmetrical features as grounding zone wedges (GZWs) and identify them as GZW01 through GZW07 (Fig. 6) representing periods of stable grounding line positions.

The deeper GZWs (GZW01, GZW02, and GZW03; Figs. 4, 6) are laterally discontinuous and show indications of erosion and disintegration. GZW01 and GZW02 extend for only ~16 km, which is about half the length of GZW04 to GZW07; whereas GZW03 is recognizable for ~28 km, although not continuously. On their southern border, GZW01 to GZW03 are limited by a glacial lobe or its morphological continuation, which shows numerous glacial lineations with a direction oblique to the prevalent strike of GZW01 to GZW03 (~NNE) and abundant iceberg keel marks (Fig. 6). GZW03 is deeper, less prominent, and irregular at its center than on its sides. The center part of GZW03 is characterized by WNW, partially exposed, and <1 km long glacial lineations (GL-05; Fig. 6). Another set of glacial lineations (GL-04; Fig. 6) is immediately west, corresponding to the northern part of GZW02 and are subparallel to GL-05 but longer (>2 km) and better preserved. In contrast, a set of glacial lineations on the northern side of GZW01 are oriented ~E-W (GL-03; Fig. 6), obliquely with respect to GL-04 and GL-05 (Fig. 6). GZW04 extends for at least 30 km, and similarly to GZW03, its central area is deeper than the sides; however, the center position of this depressed part of GZW04 is ~4 km off to the south in respect to GZW03. Unlike GZW03, GZW04 does not show signs of GLs on its surface.

In contrast to GZW01-GZW04, GZW05 has a surface of the same height with no streamline features. The absence of GLs indicates that GZW05 was neither overridden nor eroded by streaming ice. Seismic images show that GZW05 exhibits progradational geometries on its downstream (WNW) side. The most conspicuous feature of GZW05, however, is its heavily iceberg-disturbed surface that is characterized

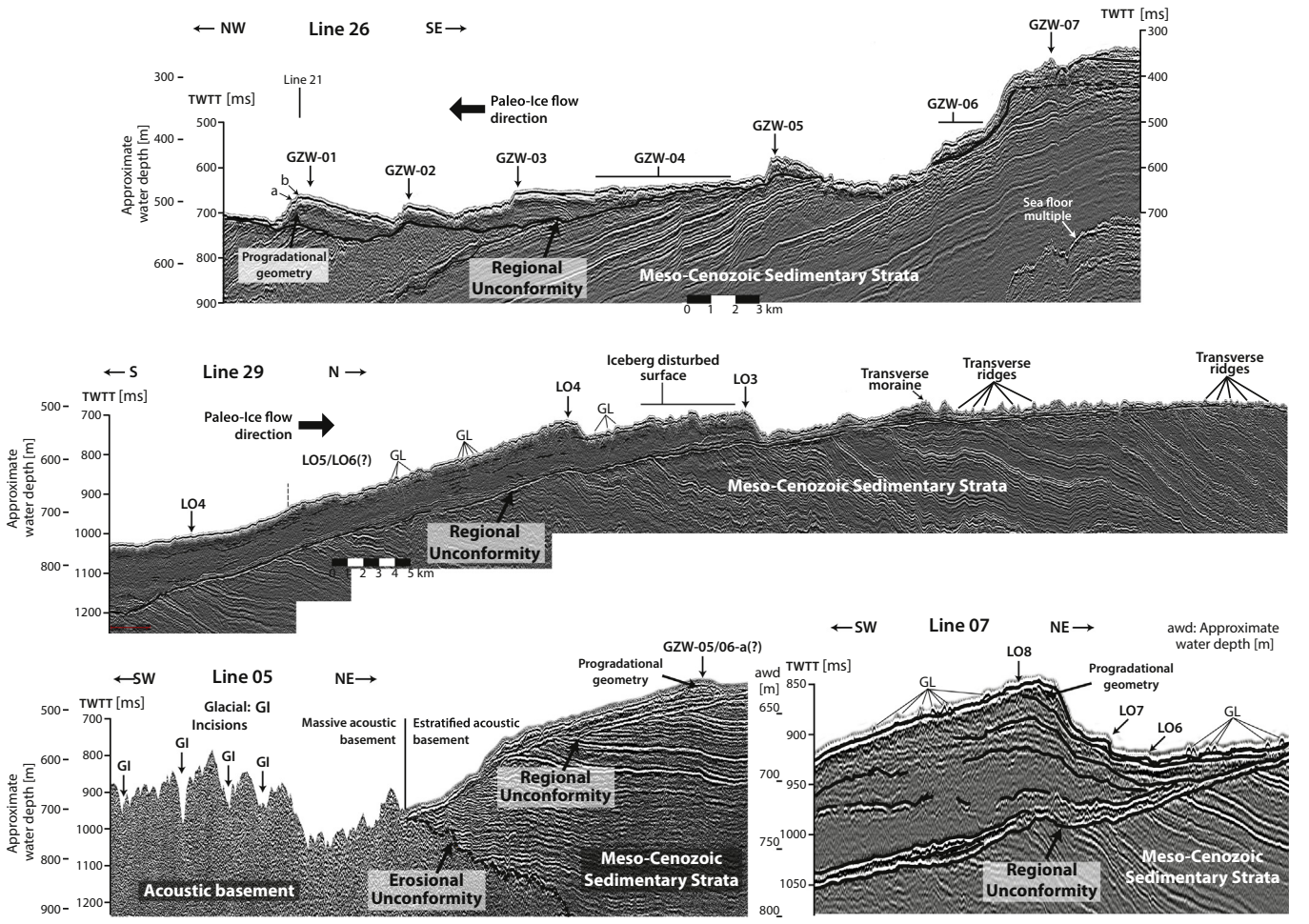

Fig. 4. Multichannel seismic lines (see Figs. 3 and 6 for location). Main reflectors and sea floor surface features are indicated, including Glacial Lobes LO04 – LO08 (Section 4.2), and Grounding Zone Wedges GZW-01 - GZW-07. Thick black arrows indicate the projection of inferred ice flow direction along the seismic lines. The Meso-Cenozoic sedimentary strata below the regional unconformity are described in Gulick et al. (2017). GL: glacial lineations; TWTT: two-way travel time.

by numerous plough marks, furrows, and keel marks, nearly all pointing NW (Fig. 6). Transverse ridges associated with GZW05 are not visible. Two GZWs, GZW5/06-a and GZW5/06-b (Fig. 6), are found just south of GZW05 in a position and in water depths between GZW05 and GZW06. Lobe GZW05/06-a has keel marks pointing north and GLs pointing NW.

GZW06 has a morphology similar to GZW04, deeper near its center and shallower on its sides; however, it lacks GLs or other evidence of erosion or deformation by streaming ice. Instead, a set of parallel ridges on its center part indicate that ice was retreating in the center part while grounded on the sides.

GZW07 is located in the shallowest part of the mapped area (~300 mbsl; Fig. 6), and it was only partially mapped because stranded icebergs prevented access to more ice proximal and shallow parts of GZW07. A conspicuous characteristic of GZW-07 are major iceberg furrows that run nearly parallel to its strike. Seismic images show signs of progradation (downlapping reflectors) and mass wasting deposits (steep slope and chaotic internal seismic architecture) on the downstream side of GZW07.

Two different sets of ridges with different orientation and geometric organization are also observed in this area. The first set, R-01 (Fig. 6), occurs west of GZW01 and is characterized by ridges oriented ~N-NW, roughly parallel to the strike of GZW01 and perpendicular to GL-03 (Fig. 6). The height of R-01 ridges is highly variable as they are often cut by iceberg furrows or plough marks; however, they usually reach ~3–5 m high while some can be up to ~10 m high, with ridge-to-ridge spacing ~100–500 m. Laterally, R-01 ridges bend, bifurcate, and merge. The R-01 ridges closer to GZW01 exhibit better continuity and narrower spacing than the ridges farther west. The second set of ridges, R-02 (Fig. 6), occurs north of GZW01. The R-02 ridges are roughly oriented NNE and perpendicular to GL-04. Near GZW01, ridges of R-02 are organized in an anastomosing pattern with some of them exhibiting wide flat tops in areas where they overlay the troughs of underlying GLs. Farther NNW from GL-04 and GL-05, R-02 ridges show a dendritic pattern diverging north, transitioning into an area where they are mostly parallel to each other. On a partially mapped area NNW of GL-03, R-02 ridges form either parallel sets oblique to the strike of R-01 ridges or form an anastomosed pattern often cut by iceberg furrows and subparallel to R-01 ridges.

3.3. The incised inner shelf

The inner shelf is characterized by a rugged sea floor incised by a relatively organized array of channels. Most of the deepest and more prominent channels are oriented subparallel to the direction of the MSGL although, locally, oblique channels can be dominant (Fig. 3). In the SW of the inner shelf area we found a set of deep (<1200 mbsl) and wide channels (<5 km), with reliefs of ~300–900 m and V- or U-shaped. This set is oriented obliquely with respect to the MSGLs (Fig. 1), while a second set of similarly shaped channels is oriented N - S and subparallel to the MSGLs but has reliefs <300 m. In the NE part, south of the glacial lobes complex, shallower but more pervasive channelization is organized in at least three sets, all of them showing relief of <300 m. The most prevalent channel set is subparallel to the MSGL,

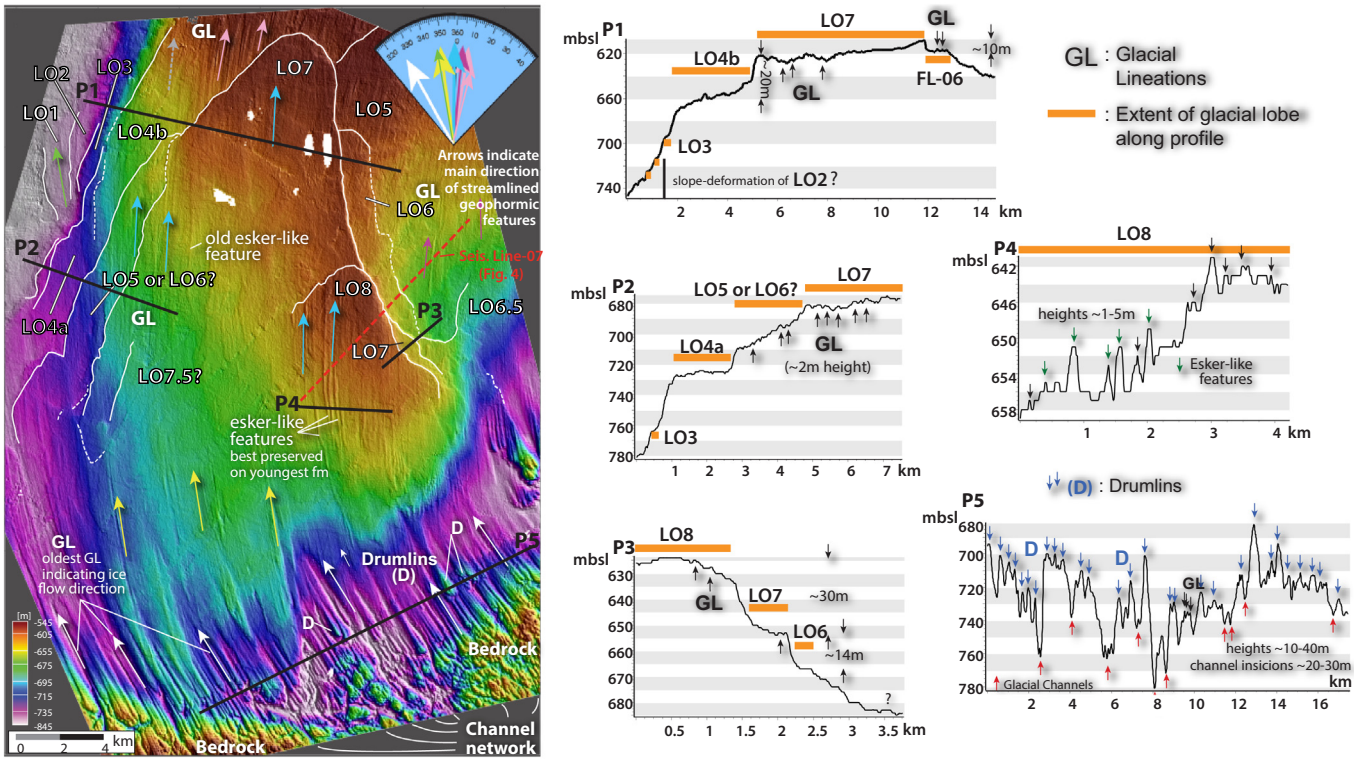

Fig. 5. Bathymetry of the glacial lobes complex area indicating the main geomorphological features. White lines indicate the glacial lobes boundaries. Color arrows indicate the direction of glacial lineations (GL) on top of glacial lobes. A comparison of GL directions (top right azimuth diagram) show that glacial lineations have different strike directions for different glacial lobes suggesting that they were formed under different ice flow conditions. Profiles P1 to P5 are based on a resampled version of the bathymetry (15 m × 15 m pixel size): the elevation difference between glacial lobes, as well as the height of glacial lineations, drumlins, and esker-like features are indicated.

while the other two sets are oriented obliquely at ~30E and 30W with respect to the MSGL (Fig. 3).

In the NE part of the inner shelf, where our mapping was more extensive (Fig. 3), seafloor morphology shows differences in the incision pattern that allow us to infer the existence of at least two types of bedrock lithology. In the eastern part of this area, channels are more deeply incised, resulting in more relief although general bathymetry is shallower (Fig. 3; S02). Comparative NNW profiles (subparallel to MSGL), show that the eastern part of this area has in general higher and more variable relief than the more uniform central and western parts (S02).

4. Interpretations and discussion

4.1. Outer shelf

The gullies of the upper continental slope along with the iceberg furrows observed near the outer shelf constitute a geomorphological association similar to other areas of the Antarctic margin, where more extensive sea floor mapping shows gullies commonly occurring just seaward of mega-scale glacial lineations at the terminus of glacial troughs or, in some cases, between them (Anderson, 1999; Shipp et al., 1999; Canals et al., 2002; Lowe and Anderson, 2002; Dowdeswell et al., 2004; Heroy and Anderson, 2005). Gullies along the Antarctic continental slope are interpreted to result from an ancient ice sheet being grounded at the shelf edge leading to meltwater sediment-laden discharge and turbidite flows down across the continental slope (Anderson, 1999). In the case of our mapped gullies, they are not spatially associated with a trough or MSGLs. Instead, they occur seaward of a relatively shallow area with grooves interpreted as iceberg keel marks and an asymmetrical promontory interpreted as representing the grounding line position of the last glacial advance to the outer shelf (Fig. 2). The proximity of a paleogrounding line and record of past iceberg activity is consistent with these gullies forming because of proximal sediment-laden meltwater discharge.

4.2. Deep middle shelf: glacial trough and glacial lobe complex

The spatial and geomorphological association, including a rugged incised inner shelf transitioning in a seaward direction toward areas with increasing sedimentary cover with drumlins and MSGLs, has been described elsewhere in Antarctica (e.g., Anderson, 1999; Heroy and Anderson, 2005; Wellner et al., 2006; Ó Cofaigh et al., 2007; Graham et al., 2009; Livingstone et al., 2012). This geomorphological association is interpreted to be the result of past grounded ice flowing from the ice sheet interior onto the continental shelf. As the ice sheet expanded over the continental shelf it would have accelerated across the transition from crystalline to sedimentary bed as the basal drag was reduced, eventually forming ice streams (Heroy and Anderson, 2005; Wellner et al., 2006; Ó Cofaigh et al., 2007; Dowdeswell et al., 2008). Abundant evidence of past ice streams on the Antarctic continental shelf is found in the form of MSGLs within glacial troughs that are usually flanked by areas with evidence of slow flowing ice (e.g., Heroy and Anderson, 2005; Wellner et al., 2006; Dowdeswell et al., 2008; Livingstone et al., 2012). We mapped a deep basin (>1000 mbsl) downstream and NW from the location of the MSGLs. In this context, the glacial lobe complex is located on the eastern side of the basin, with the GZWs on a shallow area characterized by slower flowing ice separated from the basin by a nearly straight boundary that runs parallel to the MSGLs. The association of a deep area with MSGLs flanked by a shallower area with GZWs with a boundary parallel to the direction of the MSGLs is interpreted as the result of erosion and deposition by past ice streams flowing rapidly through glacial troughs with areas of slower ice flow on the sides (Ottesen and Dowdeswell, 2009;

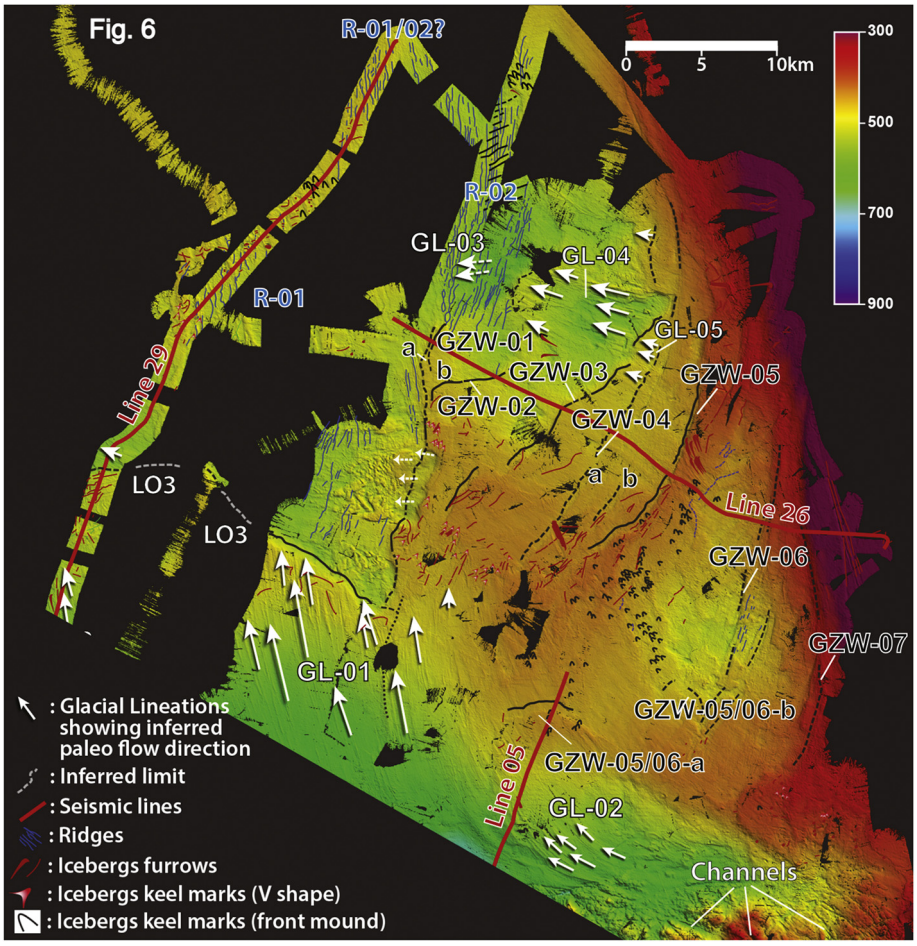

Fig. 6. Bathymetry of the shallow middle shelf area indicating the main geomorphological features. White arrows indicate the inferred ice flow direction based on the orientation of glacial lineations. Red lines show the location of the seismic lines shown in Fig. 4. Blue lines represent the crest of transverse ridges. Iceberg furrows and different shapes of keel marks are also indicated.

Batchelor and Dowdeswell, 2016). Although heavy sea ice limited any mapping farther west and based on the similarities with other areas with better coverage and our understanding of geomorphological associations, we interpret the partially mapped deep basin as the southern end of a cross-shelf glacial trough through which ice flowed as ice streams, forming MSGLs. In this scenario, the preservation of glacial lobes and GZWs can be attributed to reduced ice speed and erosion relative to the main glacial pathway within the cross-shelf trough. The presence of such a glacial trough is not well resolved by the BEDMAP2 model, although greater average depths are indicated seaward from the mapped area in the direction of the MSGLs (Fig. 3).

The glacial lobes, which overlay the MSGLs, were formed subsequently and represent periods of different ice flow configuration. The glacial lineations on the surface of the lobes and the fact that the lobes themselves are elongated in the same direction indicate that these features were formed by grounded ice flowing north with probably faster ice speeds in the center relative to the side of each glacial lobe. The stacked geometry, decreasing size, and water depth at which these lobes are found suggest that the glacial lobes were formed by successively thinner ice. The ice that formed the glacial lobes had a general main axial flow direction (NW-NNW) through the different stages that formed the glacial lobes complex but was limited in the areal coverage of each lobe by increased buoyancy. The formation of the features observed on the surface of each glacial lobe is interpreted as related to partially grounded ice that developed late in the deglacial or retreat stage of different glacial cycles or stages, since they lack signs of erosion or deformation related to thickening or advancing grounded ice. Further, it is important to note that contact with the bed was indeed maintained for a protracted period of time, leading to the stacking and aggregational/progradational characteristics of the glacial lobe-complex (see progradational geometries imaged on the downstream slope of the lobes; Fig. 4). This enduring contact means that the system must have been supplied by sufficient sediment during the decoupling process, perhaps through periodic addition of sediment-laden meltwater, to allow the lobes to keep up with thinning ice and to grow, overprinting the geographically pervasive MSGLs.

The following observations also point to the past presence of an active subglacial meltwater system. First, the prominent positive-relief glacial lineations (1–5 m high) observed on the surface of LO8 (Fig. 5) have variations in shape and strike (such as flattening, widening, and bending in directions oblique to other glacial lineations) that cannot be explained by local changes in ice flow pattern. We find similarities between these features and eskers described in terrains deglaciated during the termination of the last glacial cycle and propose that the positive relief glacial lineations of LO8 were formed by sediment deposition inside R-type channels (e.g., Clark and Walder, 1994; Walder and Fowler, 1994). This interpretation requires that a well-organized subglacial drainage system was in place at least during the last stage of formation of LO8 and provides a mechanism for sediment transport and formation of the described glacial features and corresponding glacial lobes. The origin of the subglacial water could be local, but it could also reflect a hydrological connection with inland subglacial systems (e.g., Wingham et al., 2006; Wright et al., 2012). The second observation corresponds to the spatial association of the glacial lobes and esker-like lineations, with a series of drumlins with over-deepened upstream and lateral sides that connect with a network of deep channels

carved in bedrock. This association suggests a genetic link by which sediment could have been transported along a subglacial meltwater system, proceeding along the observed bedrock channels and the drumlins field, to end up accumulated in the glacial lobes or released to ocean processes at the grounding line. The hydrological processes involved could include subglacial outburst floods (e.g., Jordan et al., 2010; Flament et al., 2014), which would explain the pervasive erosion of the bedrock, lateral incision of drumlins, and the discrete nature of the glacial lobe complex. However, we lack direct evidence of this hypothesized sediment path, and other processes such as localized glacial erosion of the sedimentary bed cannot be discarded as at least a partial source of the sediments composing the lobes.

4.3. Shallow middle shelf: grounding zone wedges (GZWs)

In marine terminating ice sheets, the position of GZWs depends strongly on the interplay between ice thickness and water depth near the grounding line that controls floatation (e.g., Gomez et al., 2010). With the exception of terminal GZWs, the preservation potential of GZWs across glacial cycles is considered low because composite GZWs are rare and overriding ice is assumed to easily erode the unconsolidated sediments comprising GZWs. In other areas of the Antarctic margin, successive GZWs are found in cross-shelf glacial troughs and interpreted as demarking ice stream still stands during glacial retreat associated with the termination of the last glacial cycle (McMullen et al., 2006; Livingstone et al., 2012; Batchelor and Dowdeswell, 2015). In these cases, preservation is achieved because glaciers have not advanced onto the continental shelf after deglaciation, and GZWs are covered by a blanket of pelagic sediments (e.g., Heroy and Anderson, 2005) that impede erosion by ocean currents. In contrast, the mapped arcuate GZWs here are not located in a glacial trough but on an inter ice stream or slow ice flow area (e.g., Ottesen and Dowdeswell, 2006; Dowdeswell et al., 2014; Batchelor and Dowdeswell, 2015). Our mapped GZWs occur at varying water depths, which we interpret as indicating that these features were constructed under different ice thickness conditions, with thinner ice corresponding to the shallower GZWs (GZW03 and shallower; Fig. 6). Preservation would be achieved because subsequent glacial advances did not have greater ice thickness and did not result in grounding line readvance. The glacial lineations and the deepening and narrowing observed in the central parts of GZW01-GZW03 (Fig. 6) indicate lateral variation in ice speed either during or shortly(?) after the construction of each respective GZW. Because the faster ice flowed through the NW-oriented cross-shelf trough (MSGL and glacial lobe complex area; Fig. 3), the glacial lineations observed on GZW01-GZW03 may indicate the initiation of fast ice flow and/or record a small ice tributary. We suggest this transition in ice flow based on the direction of glacial lineations that converge to the west. We lack absolute chronological control for the GZWs; however, based on the different water depths at which these wedges occur and their preservation, we propose a relative chronology in which age is younger for the shallower GZWs. Thus, our interpretation is that the GZWs represent either glacial thinning and retreat during one or more stages within the last glacial cycle or represent several glacial cycles of a successively thinner marginal ice sheet.

We identify a morphological association between GZWs, ridges, iceberg furrows, and GLs that can explain their geographical distribution and establish a genetic link between these features. The R-01 ridges are roughly parallel to GZW01 and perpendicular to GL-03. This geometry suggests that R-01 ridges represent recessional features formed during steady and relatively slow retreat of the grounding line until it stabilized to construct GZW01. In this scenario, GL-03 records the direction of ice flow during retreat, while the ice furrows disrupting R-01 ridges record iceberg calving, drifting, and grounding from the retreating ice front. We note that several iceberg keel marks are oblique to R-01 ridges and may indicate the calving of an ice front within an embayment, probably formed as the result of retreat of the termini of the ice stream flowing through the glacial trough, while slower ice was still grounded on GZW01 and/or GZW02. Another possibility is that calved icebergs drifted away and then moved back toward the ice front by local ocean currents or winds, where they were stranded. GZW02, which is shallower and partially overlaps GZW01, was formed subsequently to GZW01, either during the same glacial retreat stage or during a different glacial cycle. In the latter scenario, R-01 ridges would likely be associated with GZW02 as preservation of relatively shallow ridges under overriding ice is unlikely. We note that the relatively restricted extent of GZW01 and GZW02 can be associated either with fast ice flow north and south or with erosion of the northern end by subsequent glacial advances. Following similar morphological arguments, R-02 ridges (which are perpendicular to GL-04 and GL-05 glacial lineations) represent recessional features formed during steady and relatively slow retreat of the grounding line until it stabilized to construct GZW03 and GZW04. In this scenario, GL-04 and GL-05 represent a record of the direction of ice flow during retreat or shortly(?) after, as the disruption of the shape of GZW03 and the depression of the central part of GL-04 area may represent erosion by overriding ice.

GZW05, in contrast with GZW01-GZW04, has no streamlined features indicating coeval or subsequent streaming ice nor has evidence of glacial erosion, and thus the interpretation is that it was formed by stabilization of slow ice flow. The heavily iceberg-disturbed surface of GZW05 (including numerous plough marks, furrows and keel marks) and the absence of transverse ridges associated with GZW05, indicate that after stabilization of the grounding line, ice receded rapidly from GZW05 by decoupling and floatation. This retreat was likely accompanied by intense calving of grounding zone icebergs that produced scouring and deformation of the grounding zone deposits (Fig. 6). Two secondary glacial lobes, GZW05/06-a, b (Fig. 6), could be related to the retreat and last grounding event that created GZW05; however, it is also possible that they formed as part of a different and more recent glacial event.

Although GZW06 has a morphology similar to GZW04, which is deeper near its center, it lacks decisive evidence of erosion or deformation by streaming ice. Some parallel ridges indicate that retreat from GZW06 was slow, and our seismic line 26 that crosses the northern part of the lobe shows downlapping geometries more consistent with sediment mass transport than a constructional wedge. However, the overall morphology indicates a consistent supply of sediment. Morphological structures perpendicular to the parallel ridges suggest some level of erosion, but we lack direct evidence. Major scours marks are observed in the seafloor on GZW07 (Fig. 6) that could be the result of recent iceberg activity. Seismic images show sediment accumulation with subhorizontal and downlapping geometries suggestive of grounding zone deposition. No ridges or streamlined features were observed on GZW07, which could indicate rapid retreat from this area or a highly disturbed seafloor where traces of grounding line morphologies have been obliterated by recent iceberg activity.

4.4. Inner shelf

The rugged morphology of the inner shelf, including deep channels representing up to ~700–900 m in relief, is interpreted to be the result of intensive glacial erosion acting over several glacial cycles. This interpretation is based on the spatial distribution of channels, which does not conform with any other known process of channel formation, the great depths, and similar appearance to glacial channels networks found elsewhere in Antarctica. This interpretation is consistent with current estimates of glacial erosivity (e.g., Fernández et al., 2016), wherein incisions of several hundred meters of relief would require focused glacial erosion acting over several glacial periods. We speculate that the straight geometry of the NNW- and ENE-oriented glacial channels might indicate a structural weakness of the bedrock where fracturing is oriented in the same direction as the channels.

We note a pattern, pervasive to the entire area south of the glacial lobes complex, characterized by northward and southward slopes distribution perpendicular to the MSGL direction (S02), which indicates that although channels and general morphology are variable, there is a similar long-term glacial erosion pattern, perhaps linked to common anisotropy in erodibility (e.g., common sets of fractures and weaknesses) independent of bedrock lithology. We note that the eastern more deeply incised bedrock area (eastern inner shelf; Fig. 3) is just south of a deepened area with abundant drumlins and generally thin sedimentary cover, whereas the shallower but more pervasively channelized area is south of the glacial lobe complex that represents an area of relatively thick glacial sedimentary cover. This geographical association hints at a process by which sediment is more effectively generated and/or transported through a pervasive, shallower subglacial channel system rather than a more focused yet deeper one.

4.5. Glacial evolution and past ice sheet-ice stream collapse

The described geomorphological associations allow us to recognize a relative sequence of different glacial configurations (Fig. 7). In this context, we define a glacial configuration in the geomorphological sense, as an identifiable glacial organization of ice flow direction, streaming fast ice versus slow ice, and a slow, fast, or stepwise retreat pattern. The interpreted glacial configurations shown in Fig. 7 are based on the spatial and time-relative association of streamlined features (glacial lineations, MSGLs, glacial lobes), cross-flow features (such as grounding zone wedges and transverse ridges), and iceberg calving features such as furrows and keel marks. We note that each glacial configuration can potentially represent a time period spanning several glacial stages or cycles because we lack proof or strong arguments to constrain the timescales involved.

Glacial configuration I (Fig. 7) is characterized by streaming ice along a cross-shelf glacial trough (assumed to be oriented parallel to MSGLs) and resulted in the formation of drumlins and MSGLs. The shallower part of the middle shelf was occupied by slow ice as the seismic data do not show evidence of buried MSGLs. We lack sufficient coverage to determine the mode of retreat from the trough, but the depth of the mapped part of the trough, preservation of MSGLs, and lack of evidence of standstills suggest that retreat was abrupt.

Glacial configuration II (Fig. 7) is characterized by fast ice streaming both north and south of GZW01 and GZW02. GZW03 was also formed in this ice configuration, but ice flow in the area of GL-05 was either short-lived or left few morphological records. The ice stream south of these GZWs within the glacial trough flowed NNW, oblique relative to the main ice flow direction of glacial configuration I, and glacial lobes FL01 through FL04 were formed during this period. The grounding line

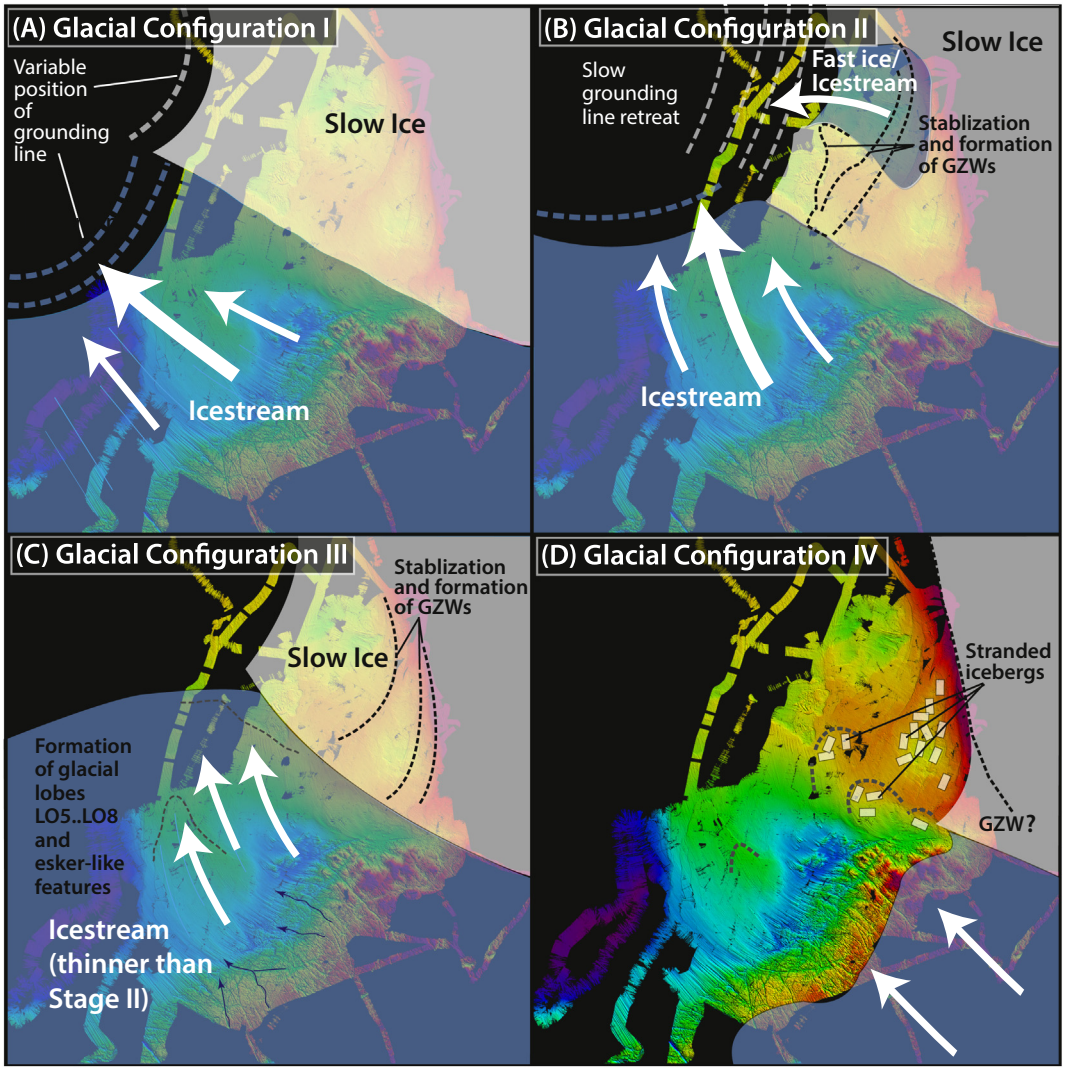

Fig. 7. Inferred past glacial stages showing different ice flow configurations, areas of fast-streaming ice (white arrows over blue), slow retreat (grey dashed lines), and position of the mapped geomorphological features (black dashed lines). White rectangles represent stranded icebergs.

retreated slowly in the western part of the middle shelf for this ice configuration leaving the two sets of ridges previously described (R-01 and R-02; Fig. 6). After the formation of GZW01-GZW03, when ice had retreated from that position, icebergs that probably calved from the retreating southern ice stream scoured the southern part of GZW01-GZW03. Although GZW04 shows no conclusive evidence of erosion or fast ice streaming, its depressed central part suggests more active glacial flow or thicker ice in that area, which would suggest that GZW04 was formed under glacial configuration II (Fig. 7). We note that GZW01 -GZW03 could correspond to different glacial stages or cycles as suggested by the different morphology and apparent degree of preservation.

Glacial configuration III (Fig. 6) is characterized by ice streaming only in the southern trough, where glacial lobes FL04 through FL08 were formed; while in the shallow middle shelf area, slow ice is associated with the formation of GZW05-GZW07. These GZWs lack glacial lineations or signs of subglacial erosion, thus suggesting that fast decoupling and/or stepwise retreat followed the formation of each GZW. Seismic line 26 (Fig. 4) shows the association of GZWs and bedrock promontories, which suggests that the position of GZWs was controlled by bed morphology. The observation of esker-like ridges on FL08 interpreted as sediment deposition in R channels, and the suggestion of erosion around drumlins just south of FL08, is interpreted as reflecting subglacial water flowing NW from the bedrock channels area into the trough. Since these esker-like features represent the last record of grounded ice activity on lobe FL08, we hypothesize a process link by which increasing hydrostatic pressure at the bed-ice interface results in increased lubrication, hence faster flow, forming R channels, and eventually resulting in dynamic thinning, ice lift off, and grounding line retreat. However, further studies are needed to test this hypothesis.

Glacial configuration IV (Fig. 7) is associated with widespread seafloor scouring by icebergs, including abundant keel and plough marks, representing the calving of large volumes of ice posterior to the formation or retreat of/from GZW05. The direction of keel marks indicates icebergs moving from east to west and from SE to NW, which might indicate widespread calving on the ice stream and on the slow ice parts of the ice margin. Because no transverse ridges were found in the areas near the keel and plough marks, we infer that ice retreat over this area occurred rapidly and resulted in calving near the grounding line, which produced icebergs thick enough to scour GZW05. We note that icebergs calved from a grounding line related to GZW07 are unlikely to be thick enough to scour the seafloor at water depths near GZW05. GZW06 could be related to the same glacial cycle as GZW05 and represent a temporary stabilization of the grounding line after retreating from GZW05, but we lack enough data to test this hypothesis. However, the lack of streamlined features on the surface of GZW05 and the preservation of keel and plough marks on its surface indicate that ice was relatively thin when grounded on GZW06 and GZW07.

The different ice flow configurations and retreat patterns observed in our study area indicate highly variable ice dynamics at the margin of the East Antarctic Ice Sheet. These dynamics include (i) the rearrangement of fast-ice flow paths, (ii) switching on and off of basal erosion and sediment deposition in different parts of the system, (iii) an active subglacial hydrological network including the possibility of subglacial outburst floods, and (iv) variable retreat modes and rates. The corollary is that present ice dynamics at the margin of the so-called stable East Antarctic Ice Sheet can change dramatically. However, the rates and timescales of these changes, as well as their main forcing, remain unconstrained.

5. Conclusions

The data presented here from the Sabrina continental shelf offshore the Aurora subglacial basin document a complex set of geomorphological features associated with varying ice dynamic conditions. Our main conclusions are:

- We find evidence that in the past, ice reached the outer shelf west of the modern Dalton Ice Tongue and grounded ~5 km from the shelf edge at ~450 mbsl, extending ~155 km north of the current coastline (Moscow University Ice Shelf), resulting in iceberg scouring of the sea floor near the shelf edge and in the formation of gullies in the upper continental slope.
- We present evidence of a NW-oriented cross-shelf trough with paleoice flow direction indicated by mega-scale glacial lineations (MSGL) and drumlins and a series or geomorphic associations, including grounding zone wedges, glacial lineations, and transverse ridges, indicating slower ice and grounding line stabilization and collapse on the northern flank of the trough. All these geomorphic features are constructed on sediments overlying a regional angular erosional unconformity that truncate tilted Meso-Cenozoic strata deposited before widespread polar glaciation in East Antarctica (Gulick et al., 2017).
- We identify four different past ice flow configurations (glacial configurations I to IV; Fig. 7: GCI-GCIV) on the inner-middle shelf area that reflect changes in ice flow direction, grounding line position, location of fast and slow ice areas, and retreat pattern. The GCI is related to the existence of a paleoice stream and formation of MSGLs in a partially mapped cross-shelf trough. The GCII is characterized by streaming ice in the trough and shallower middle shelf on the right flank of the trough. The streaming ice in the trough resulted in sediment deposition and the partial burial of MSGLs by glacial lobes. The ice on the flank of the trough was accompanied by the formation of at least three grounding zone wedges (GZWs), as result of slower ice between the fast-streaming ice. The GCIII is characterized by thinner ice than the previous glacial configurations, and ice streaming only in the cross-shelf trough, with further ice grounding and sediment accumulation on the glacial lobes. Slower ice in the northern flank of the trough and shallower middle shelf, stabilized to form three to four GZWs at different water depths, implying continued thinning of the overriding ice for the wedges. The GCIV is associated with fast grounding line retreat and high rates of near grounding line calving. It is related to the formation and retreat from GZW05 and perhaps the shallowest glacial lobe in the trough area, as well as probably GZW06, all perhaps occurring within the same glacial cycle although further studies are needed to resolve the timing of these events. The identification of several different ice flow configurations indicates a dynamic ice sheet margin with varying glacial conditions and retreat modes. If GZWs were formed during different glacial stages or cycles, then the inferred diminishing ice thickness for consecutive grounding zone wedges suggests that the margin of the Antarctic ice sheet has evolved to a less extensive coverage of the continental shelf through successive cycles.
- We observe that this part of the EAIS margin holds morphological features similar to those found in the Amundsen Sea sector of the West Antarctic Ice Sheet (WAIS) where they are associated with ice sheet and ice stream expansion and subsequent retreat or collapse (e.g., streamlined features such as MSGLs, iceberg furrows, GZWs, plough marks, and seafloor scouring). The association of these features in our study area suggests the possibility of rapid grounding line retreat and high rates of near grounding-line calving, indicating that the EAIS margin can behave as dynamically as the WAIS margin.
- We find evidence of sediment deposition in the form of ridges subparallel or oblique with respect to coeval glacial lineations, described as esker-like ridges, consistent with the existence of R-channels in the formation of the glacial (glacial) lobes described in the trough area. This observation, along with morphological evidence of erosion surrounding drumlins south of the esker-like ridges, indicates the presence of an organized subglacial hydrological system during the last stage of formation of the glacial lobes. The spatial association of these features with a network of deep incisions on the bedrock of the inner shelf suggests a genetic link. We hypothesize that sediment could have been transported through a network of bedrock-incised

subglacial channels toward the margin of the ice sheet. It is possible that this subglacial hydrological system was at least intermittently connected to the Aurora Basin, including the possibility of recurrent subglacial outburst flooding events; further studies are needed to test this hypothesis.

Acknowledgements

We thank the NBP14-02 science party, ECO crew, and ASC staff aboard the RV/IBV N.B. Palmer for their help during the geophysical survey. NBP14-02 was supported by National Science Foundation grants PLR-1143836, -1143837, -1143843, -1430550, and -1048343. We also thank the team of marine mammal observers that insured that seismic operations were done safely for the local marine life. We thank Richard A. Marston, editor in chief of Geomorphology, and Ian S. Evans who reviewed the manuscript for their insightful comments. This is UTIG contribution #3273.

Appendix A. Supplementary data

Supplementary data to this article can be found online at https://doi.org/10.1016/j.geomorph.2018.05.020.

References

Aitken, A.R.A., Young, D.A., Ferraccioli, F., Betts, P.G., Greenbaum, J.S., Richter, T.G., Roberts, J.L., Blankenship, D.D., Siegert, M.J., 2014. The subglacial geology of Wilkes Land, East Antarctica. Geophys. Res. Lett. 41:2390–2400. https://doi.org/10.1002/2014GL059405.

Aitken, A.R.A., Roberts, J.L., Van Ommen, T.D., Young, D.A., Golledge, N.R., Greenbaum, J.S., Blankenship, D.D., Siegert, M.J., 2016. Repeated large-scale retreat and advance of Totten Glacier indicated by inland bed erosion. Nature 533:385–389. https://doi.org/10.1038/nature17447.

Anderson, J.B., 1999. Antarctic Marine Geology. Cambridge University Press, Cambridge.

Batchelor, C.L., Dowdeswell, J.A., 2015. Ice-sheet grounding-zone wedges (GZWs) on high-latitude continental margins. Mar. Geol. 363:65–92. https://doi.org/10.1016/j.margeo.2015.02.001.

Batchelor, C.L., Dowdeswell, J.A., 2016. Lateral shear-moraines and lateral marginal-moraines of palaeo-ice streams. Quat. Sci. Rev. 151:1–26. https://doi.org/10.1016/j.quascirev.2016.08.020.

Beaman, R.J., O'Brien, P.E., Post, A.L., Santis, L.D., 2011. A new high-resolution bathymetry model for the Terre Adélie and George V continental margin, East Antarctica. Antarct. Sci. 23 (1):95–103. https://doi.org/10.1017/S095410201000074X.

Canals, M., Casamor, J.L., Urgeles, R., Calafat, A.M., Domack, E.W., Baraza, J., Farran, M., De Batist, M., 2002. Seafloor evidence of a subglacial sedimentary system off the northern Antarctic Peninsula. Geology 30 (7):603–606. https://doi.org/10.1130/0091-7613.

Chen, J.L., Wilson, C.R., Blankenship, D., Tapley, B.D., 2009. Accelerated Antarctic ice loss from satellite gravity measurements. Nat. Geosci. 2:859–862. https://doi.org/10.1038/NGEO694.

Clark, P.U., Walder, J.S., 1994. Subglacial drainage, eskers, and deforming beds beneath the Laurentide and Eurasian ice sheets. Geol. Soc. Am. Bull. 106, 304–314.

Clark, P.U., Dyke, A.S., Shakun, J.D., Carlson, A.E., Clark, J., Wohlfarth, B., Mitrovica, J.X., Hostetler, S.W., McCabe, A.M., 2009. The Last Glacial Maximum. Science 325: 710–714. https://doi.org/10.1126/science.1172873.

DeConto, R.M., Pollard, D., 2016. Contribution of Antarctica to past and future sea-level rise. Nature 531:591–597. https://doi.org/10.1038/nature17145.

Dowdeswell, J.A., Ó Cofaigh, C., Pudsey, C.J., 2004. Continental slope morphology and sedimentary processes at the mouth of an Antarctic palaeo-ice stream. Mar. Geol. 204, 203–214.

Dowdeswell, J.A., Ó Cofaigh, C., Noormets, R., Larter, R.D., Hillenbrand, C.D., Benetti, S., Evans, J., Pudsey, C.J., 2008. A major trough-mouth fan on the continental margin of the Bellingshausen Sea, West Antarctica: the Belgica Fan. Mar. Geol. 252:129–140. https://doi.org/10.1016/j.margeo.2008.03.017.

Dowdeswell, J.A., Hogan, K.A., Ó Cofaigh, C., Fugelli, E.M.G., Evans, J., Noormets, R., 2014. Late Quaternary ice flow in a West Greenland fjord and cross-shelf trough system: submarine landforms from Rink Isbrae to Uummannaq shelf and slope. Quat. Sci. Rev. 92:292–309. https://doi.org/10.1016/j.quascirev.2013.09.007.

Evans, J., Dowdeswell, J.A., O Cofaigh, C., Benham, T.J., Anderson, J.B., 2006. Extent and dynamics of the West Antarctic Ice Sheet on the outer continental shelf of Pine Island Bay during the last glaciation. Mar. Geol. 230:53–72. https://doi.org/10.1016/j.margeo.2006.04.001.

Fernández, R., Anderson, J.B., Wellner, J.S., Minzoni, R.L., Hallet, B., 2016. Latitudinal variation in glacial erosion rates from Patagonia and the Antarctic Peninsula (46°–65° S). Geol. Soc. Am. Bull. 128 (5–6):1000–1023. https://doi.org/10.1130/B31321.1.

Flament, T., Berthier, E., Remy, F., 2014. Cascading water underneath Wilkes Land, East Antarctic ice sheet, observed using altimetry and digital elevation models. Cryosphere 8:673–687. https://doi.org/10.5194/tc-8-673-2014.

Fretwell, P., Pritchard, H.D., Vaughan, D.G., Bamber, J.L., Barrand, N.E., Bell, R., Bianchi, C., Bingham, R.G., Blankenship, D.D., Casassa, G., Catania, G., Callens, D., Conway, H., Cook, A.J., Corr, H.F.J., Damaske, D., Damm, V., Ferraccioli, F., Forsberg, R., Fujita, S., Gim, Y., Gogineni, P., Griggs, J.A., Hindmarsh, R.C.A., Holmlund, P., Holt, J.W., Jacobel, R.W., Jenkins, A., Jokat, W., Jordan, T., King, E.C., Kohler, J., Krabill, W., Riger-Golledge, N.R., Fogwill, C.J., Mackintosh, A.N., Buckley, K.M., 2012. Dynamics of the last glacial maximum Antarctic ice-sheet and its response to ocean forcing. Proc. Natl. Acad. Sci. 109 (40):16052–16056. https://doi.org/10.1073/pnas.1205385109.

Fretwell, P., Pritchard, H.D., Vaughan, D.G., Bamber, J.L., Barrand, N.E., Bell, R., Bianchi, C., Bingham, R.G., Blankenship, D.D., Casassa, G., Catania, G., Callens, D., Conway, H., Cook, A.J., Corr, H.F.J., Damaske, D., Damm, V., Ferraccioli, F., Forsberg, R., Fujita, S., Gim, Y., Gogineni, P., Griggs, J.A., Hindmarsh, R.C.A., Holmlund, P., Holt, J.W., Jacobel, R.W., Jenkins, A., Jokat, W., Jordan, T., King, E.C., Kohler, J., Krabill, W., Riger-Kusk, M., Langley, K.A., Leitchenkov, G., Leuschen, C., Luyendyk, B.P., Matsuoka, K., Mouginot, J., Nitsche, F.O., Nogi, Y., Nost, O.A., Popov, S.V., Rignot, E., Rippin, D.M., Rivera, A., Roberts, J., Ross, N., Siegert, M.J., Smith, A.M., Steinhage, D., Studinger, M., Sun, B., Tinto, B.K., Welch, B.C., Wilson, D., Young, D.A., Xiangbin, C., Zirizzotti, A., 2013. Bedmap2: improved ice bed, surface and thickness datasets for Antarctica. Cryosphere 7:375–393. https://doi.org/10.5194/tc-7-375-2013.

Golledge, N.R., Kowalewski, D.E., Naish, T.R., Levy, R.H., Fogwill, C.J., Gasson, E.G.W., 2015. The multi-millennial Antarctic commitment to future sea-level rise. Nature 526: 421–425. https://doi.org/10.1038/nature15706.

Gomez, N., Mitrovica, J.X., Huybers, P., Clark, P.U., 2010. Sea level as a stabilizing factor for marine-ice-sheet grounding lines. Nat. Geosci. 3:850–853. https://doi.org/10.1038/ngeo1012.

Graham, A.G.C., Larter, R.D., Gohl, K., Hillenbrand, C.-D., Smith, J.A., Kuhn, G., 2009. Bedform signature of a West Antarctic palaeo-ice stream reveals a multi-temporal record of flow and substrate control. Quat. Sci. Rev. 28:2774–2793. https://doi.org/10.1016/j.quascirev.2009.07.003.

Gulick, S.P.S., Montelli, A., Shevenell, A., Fernandez, R., Smith, C., Warny, S., Sjunneskog, C., Bohaty, S., Leventer, A., Blankenship, D., Frederick, B., 2017. Initiation and long-term instability of the East Antarctic Ice Sheet. Nature 552:225–229. https://doi.org/10.1038/nature25026.

Hanna, E., Navarro, F.J., Pattyn, F., Domingues, C.M., Fettweis, X., Ivins, E.R., Nicholls, R.J., Ritz, C., Smith, B., Tulaczyk, S., Whitehouse, P.L., Zwally, H.J., 2013. Ice-sheet mass balance and climate change. Nature 498:51–59. https://doi.org/10.1038/nature12238.

Heroy, D.C., Anderson, J.B., 2005. Ice-sheet extent of the Antarctic Peninsula region during the Last Glacial Maximum (LGM)—insights from glacial geomorphology. Geol. Soc. Am. Bull. 117, 1497–1512.

Ivins, E.R., James, T.S., Wahr, J., Schrama, E.J.O., Landerer, F.W., Simon, K.M., 2013. Antarctic contribution to sea level rise observed by GRACE with improved GIA correction. J. Geophys. Res. Solid Earth 118:3126–3141. https://doi.org/10.1002/jgrb.50208.

Jakobsson, M., Anderson, J.B., Nitsche, F., Dowdeswell, J., Gyllencreutz, R., Kirchner, N., Mohammad, R., O'Regan, M., Anandakrishnan, S., Alley, R.B., Eriksson, B., Kirshner, A., Fernández, R., Stolldorf, T., Minzoni, R., Majewski, W., 2011. Geological record of ice shelf break-up and grounding line retreat, Pine Island Bay, West Antarctica. Geology 39:691–694. https://doi.org/10.1130/G32153.1.

Jezek, K.C., RAMP Product Team, 2002. RAMP AMM-1 SAR Image Mosaic of Antarctica. Alaska SAR Facility, Fairbanks, AK (association with the National Snow and Ice Data Center, Boulder, CO. Digital media). http://nsidc.org/data/docs/daac/nsidc0103_ramp_mosaic.gd.html.

Jordan, T.A., Ferraccioli, F., Corr, H., Graham, A., Armadillo, E., Bozzo, E., 2010. Hypothesis for mega-outburst flooding from a palaeo-subglacial lake beneath the East Antarctic Ice Sheet. Terra Nova 22:283–289. https://doi.org/10.1111/j.1365-3121.2010.00944.x.

Kingslake, J., Ely, J.C., Das, I., Bell, R.E., 2017. Widespread movement of meltwater onto and across Antarctic ice shelves. Nature 544:349–352. https://doi.org/10.1038/nature22049.

Lavoie, C., Domack, E.W., Pettit, E.C., Scambos, T.A., Larter, R.D., Schenke, H.W., Yoo, K.C., Gutt, J., Wellner, J., Canals, M., Anderson, J.B., Amblas, D., 2015. Configuration of the Northern Antarctic Peninsula Ice Sheet at LGM based on a new synthesis of seabed imagery. Cryosphere 9:1–16. https://doi.org/10.5194/tc-9-1-2015.

Lenaerts, J.T.M., Vizcaino, M., Fyke, J., Kampenhout, L.V., Broeke, M.R., 2016. Present-day and future Antarctic ice sheet climate and surface mass balance in the Community Earth System Model. Clim. Dyn. 47:1367–1381. https://doi.org/10.1007/s00382-015-2907-4.

Leventer, A., Domack, E., Dunbar, R., Pike, J., Stickley, C., Maddison, E., Brachfeld, S., Manley, P., McClennen, C., 2006. Marine sediment record from the East Antarctic margin reveals dynamics of ice sheet recession. GSA Today 16:12. https://doi.org/10.1130/GSAT01612A.

Li, X., Rignot, E., Mouglnot, J., Scheuchl, B., 2016. Ice flow dynamics and mass loss of Totten Glacier, East Antarctica, from1989 to 2015. Geophys. Res. Lett. 43: 6366–6373. https://doi.org/10.1002/2016GL069173.

Livingstone, S.J., O Cofaigh, C., Stokes, C.R., Hillenbrand, C., Vieli, A., Jamieson, S.S.R., 2012. Antarctic palaeo-ice streams. Earth Sci. Rev. 111:90–128. https://doi.org/10.1016/j.earscirev.2011.10.003.

Lowe, A.L., Anderson, J.B., 2002. Reconstruction of the West Antarctic Ice Sheet in Pine Island Bay during the Last Glacial Maximum and its subsequent retreat history. Quat. Sci. Rev. 21:1879–1897. https://doi.org/10.1016/S0277-3791(02)00006-9.

Lowe, A.L., Anderson, J.B., 2003. Evidence for abundant subglacial meltwater beneath the paleo-ice sheet in Pine Island Bay, Antarctica. J. Glaciol. 49 (164), 125–138.

Lythe, M.B., Vaughan, D.G., BEDMAP Consortium, 2001. BEDMAP- a new ice thickness and subglacial topographic model of Antarctica. J. Geophys. Res. 106 (B6), 11335–11351.

Mackintosh, A.N., Golledge, N., Domack, E., Dunbar, R., Leventer, A., White, D., Pollard, D., DeConto, R., Fink, D., Zwartz, D., Gore, D., Lavoie, C., 2011. Retreat of the East Antarctic ice sheet during the last glacial termination. Nat. Geosci. 4:195–202. https://doi.org/10.1038/ngeo1061.

Mackintosh, A.N., Verleyen, E., O'Brien, P.E., White, D.A., Jones, R.S., McKay, R., Dunbar, R., Gore, D.B., Fink, D., Post, A.L., Miura, H., Leventer, A., Goodwin, I., Hodgson, D.A., Lilly, K., Crosta, X., Golledge, N.R., Wagner, B., Berg, S., Ommeno, T., Zwartz, D., Roberts, S.J., Vyverman, W., Masse, G., 2014. Retreat history of the East Antarctic Ice Sheet since the Last Glacial Maximum. Quat. Sci. Rev. 100:10–30. https://doi.org/10.1016/j.quascirev.2013.07.024.

Maclachlan, J.C., Eyles, C.H., 2013. Quantitative geomorphological analysis of drumlins in the Peterborough drumlin field, Ontario, Canada. Geogr. Ann. 95 (2):125–144. https://doi.org/10.1111/geoa.12005.

McMullen, K., Domack, E., Leventer, A., Olson, C., Dunbar, R., Brachfeld, S., 2006. Glacial morphology and sediment formation in the Mertz Trough, East Antarctica. Palaeogeogr. Palaeoclimatol. Palaeoecol. 231:169–180. https://doi.org/10.1016/j.palaeo.2005.08.004.

Nitsche, F.O., Gohl, K., Larter, R.D., Hillenbrand, C.D., Kuhn, G., Smith, J.A., Jacobs, S., Anderson, J.B., Jakobsson, M., 2013. Paleo ice flow and subglacial meltwater dynamics in Pine Island Bay, West Antarctica. Cryosphere 7:249–262. https://doi.org/10.5194/tc-7-249-2013.

Ó Cofaigh, C., Evans, J., Dowdeswell, J.A., Larter, R.D., 2007. Till characteristics, genesis and transport beneath Antarctic paleo-ice streams. J. Geophys. Res. 112, F03006. https://doi.org/10.1029/2006JF000606.

O'Brien, P.E., Beaman, R., De Santis, L., Domack, E.W., Escutia, C., Harris, P.T., Leventer, A., McMullen, K., Post, A., Quilty, P.G., Shevenell, A.E., Batchelor, C.L., 2016. Submarine glacial landforms on the cold East Antarctic margin. Geol. Soc. Lond. Mem. 46: 501–508 2016. https://doi.org/10.1144/M46.172.

Ottesen, D., Dowdeswell, J.A., 2006. Assemblages of submarine landforms produced by tidewater glaciers in Svalbard. J. Geophys. Res. 111, F01016. https://doi.org/10.1029/2005JF000330.

Ottesen, D., Dowdeswell, J.A., 2009. An inter–ice-stream glaciated margin: submarine landforms and a geomorphic model based on marine-geophysical data from Svalbard. Geol. Soc. Am. Bull. 121 (11/12):1647–1665. https://doi.org/10.1130/B26467.1.

Pingree, K., Lurie, M., Hughes, T., 2011. Is the East Antarctic ice sheet stable? Quat. Res. 75: 417–429. https://doi.org/10.1016/j.yqres.2010.12.001.

Pritchard, H.D., Ligtenberg, S.R.M., Fricker, H.A., Vaughan, D.G., Van Den Broeke, M.R., Padman, L., 2012. Antarctic ice-sheet loss driven by basal melting of ice shelves. Nature 484:502–505. https://doi.org/10.1038/nature10968.

Reconstruction of Antarctic Ice Sheet Deglaciation (RAISED) Consortium, 2014. A community-based geological reconstruction of Antarctic Ice Sheet deglaciation since the Last Glacial Maximum. Quat. Sci. Rev. 100:1–9. https://doi.org/10.1016/j.quascirev.2014.06.025.

Rignot, E., Casassa, G., Gogineni, P., Krabill, W., Rivera, A., Thomas, R., 2004. Accelerated ice discharge from the Antarctic Peninsula following the collapse of Larsen B ice shelf. Geophys. Res. Lett. 31, L18401. https://doi.org/10.1029/2004GL020697.

Rignot, E., Bamber, J.L., Van Den Broeke, M.R., Davis, C., Li, Y., Van De Berg, W.J., Van Meijgaard, E., 2009. Recent Antarctic ice mass loss from radar interferometry and regional climate modelling. Nat. Geosci. 1, 106–110.

Rignot, E., Jacobs, S., Mouginot, J., Scheuchl, B., 2013. Ice shelf melting around Antarctica. Science 341 (6143):266–270. https://doi.org/10.1126/science.1235798.

Rintoul, S.R., Silvano, A., Pena-Molino, B., Wijk, E.V., Rosenberg, M., Greenbaum, J.S., Blankenship, D.D., 2016. Ocean heat drives rapid basal melt of the Totten Ice Shelf. Sci. Adv. 2, e1601610. https://doi.org/10.1126/sciadv.1601610.

Rott, H., Rack, W., Skvarca, P., De Angelis, H., 2002. Northern Larsen Ice Shelf, Antarctica: further retreat after collapse. Ann. Glaciol. 34, 277–282.

Scambos, T.A., Bohlander, J.A., Shuman, C.A., Skvarca, P., 2004. Glacier acceleration and thinning after ice shelf collapse in the Larsen B embayment, Antarctica. Geophys. Res. Lett. 31 (18), L18402. https://doi.org/10.1029/2004GL020670.

Shipp, S., Anderson, J.B., Domack, E.W., 1999. Late Pleistocene-Holocene retreat of the West Antarctic ice-sheet system in the Ross Sea; part 1, geophysical results. Geol. Soc. Am. Bull. 111 (10), 1486–1516.

Siegert, M.J., Carter, S., Tabacco, I., Popov, S., Blankenship, D.D., 2005. A revised inventory of Antarctic subglacial lakes. Antarct. Sci. 17 (3):453–460. https://doi.org/10.1017/S0954102005002889.

Siegfried, M.R., Fricker, H.A., Carter, S.P., Tulaczyk, S., 2016. Episodic ice velocity fluctuations triggered by a subglacial flood in West Antarctica. Geophys. Res. Lett. 43:2640–2648. https://doi.org/10.1002/2016GL067758.

Smith, J.A., Hillenbrand, C., Larter, R.D., Graham, A.G.C., Kuhn, G., 2009. The sediment infill of subglacial meltwater channels on the West Antarctic continental shelf. Quat. Res. 71:190–200. https://doi.org/10.1016/j.yqres.2008.11.005.

Spagnolo, M., Clark, C.D., Hughes, A.L.C., Dunlop, P., 2011. The topography of drumlins; assessing their long profile shape. Earth Surf. Process. Landf. 36:790–804. https://doi.org/10.1002/esp.2107.

Stearns, L.A., Smith, B.E., Hamilton, G.S., 2008. Increased flow speed on a large East Antarctic outlet glacier caused by subglacial floods. Nat. Geosci. 1:827–831. https://doi.org/10.1038/ngeo356.

Walder, J.S., Fowler, A., 1994. Channelized subglacial drainage over a deformable bed. J. Glaciol. 40 (134), 3–15.

Wellner, J.S., Heroy, D.C., Anderson, J.B., 2006. The death mask of the Antarctic ice sheet: comparison of glacial geomorphic features across the continental shelf. Geomorphology 75, 157–171.

Wingham, D.J., Siegert, M.J., Shepherd, A., Muir, A.S., 2006. Rapid discharge connects Antarctic subglacial lakes. Nature 440:1033–1036. https://doi.org/10.1038/nature04660.

Witus, A.E., Branecky, C.M., Anderson, J.B., Szczucinski, W., Schroeder, D.M., Blankenship, D.D., Jakobsson, M., 2014. Meltwater intensive glacial retreat in polar environments and investigation of associated sediments: example from Pine Island Bay, West Antarctica. Quat. Sci. Rev. 85:99–118. https://doi.org/10.1016/j.quascirev.2013.11.021.

Wright, A.P., Young, D.A., Roberts, J.L., Schroeder, D.M., Bamber, J.L., Dowdeswell, J.A., Young, N.W., Le Brocq, A.M., Warner, R.C., Paynbe, A.J., Blankenship, D.D., Van Ommen, T.D., Siegert, M.J., 2012. Evidence of a hydrological connection between the ice divide and ice sheet margin in the Aurora Subglacial Basin, East Antarctica. J. Geophys. Res. 117, F01033. https://doi.org/10.1029/2011JF002066.

Young, D.A., Wright, A.P., Roberts, J.L., Warner, R.C., Young, N.W., Greenbaum, J.S., Schroeder, D.M., Holt, J.W., Sugden, D.E., Blankenship, D.D., Van Ommen, T.D., Siegert, M.J., 2011. A dynamic early East Antarctic Ice Sheet suggested by ice-covered fjord landscapes. Nature 474:72–75. https://doi.org/10.1038/nature10114.

Zwally, H.J., Li, J., Robbins, J.W., Saba, J.L., Yi, D., Brenner, A.C., 2015. Mass gains of the Antarctic ice sheet exceed losses. J. Glaciol. 61 (230):1019–1036. https://doi.org/10.3189/2015JoG15J071.